JACS
JOURNAL OF THE AMERICAN CHEMICAL SOCIETY
Communication
pubs.acs.org/JACS

Significant Expansion of Fluorescent Protein Sensing Ability through the Genetic Incorporation of Superior Photo-Induced Electron-Transfer Quenchers

Xiaohong Liu,[†,∥] Li Jiang,[†,∥] Jiasong Li,[†,∥] Li Wang,[†] Yang Yu,[‡] Qing Zhou,[†] Xiaoxuan Lv,[†] Weimin Gong,[†] Yi Lu,[§] and Jiangyun Wang*[,†]

[†]Laboratory of RNA Biology, Institute of Biophysics, Chinese Academy of Sciences, Chaoyang District, Beijing, 100101, China
[§]Center of Biophysics and Computational Biology and Department of Chemistry, University of Illinois at Urbana−Champaign, Urbana, Illinois 61801, United States
[‡]Tianjin Institute of Industrial Biotechnology, Chinese Academy of Sciences, Tianjin 300308, China

Supporting Information

ABSTRACT: Photo-induced electron transfer (PET) is ubiquitous for photosynthesis and fluorescent sensor design. However, genetically coded PET sensors are underdeveloped, due to the lack of methods to site-specifically install PET probes on proteins. Here we describe a family of acid and Mn(III) turn-on fluorescent protein (FP) sensors, named iLovU, based on PET and the genetic incorporation of superior PET quenchers in the fluorescent flavoprotein iLov. Using the iLovU PET sensors, we monitored the cytoplasmic acidification process, and achieved Mn(III) fluorescence sensing for the first time. The iLovU sensors should be applicable for studying pH changes in living cells, monitoring biogentic Mn(III) in the environment, and screening for efficient manganese peroxidase, which is highly desirable for lignin degradation and biomass conversion. Our work establishes a platform for many more protein PET sensors, facilitates the *de novo* design of metalloenzymes harboring redox active residues, and expands our ability to probe protein conformational dynamics.

Genetically encoded, fluorescent protein (FP) sensors and imaging agents are an important part of the chemical tool box for biological studies.[1−7] PET is the most widely employed mechanism for the design of small molecule fluorescent sensors,[6,7] due to the large fluorescence enhancement (10−100-fold are typical) upon analyte binding. However, such PET sensors can be difficult to synthesize and are not easily targetable to specific locations of cells or animal tissues.

The modular fluorophore-spacer-receptor format is highly successful for designing PET fluorescent sensors (Figure S1).[6] In ligand-free and "OFF" state, photoexcitation of the fluorophore results in electron transfer (ET) between the receptor and the fluorophore, dissipating the light energy and quenching the fluorescence signal. In "ON" state, ligand binding to receptor significantly decreases the HOMO energy of the receptor, arresting the PET process and allowing the fluorophore to emit photons.

To design genetically encoded PET sensors, here we report the efficient genetic incorporation of five UAA tyrosine analogues as environmental sensitive PET probes (Figure 1): 3-chlorotyrosine (ClY), 3,5-dichlorotyrosine (Cl2Y), 3,5-fluorotyrosine (F2Y), 2,3,5-trifluorotyrosine (F3Y), 2,3,5,6-trifluorotyrosine (F4Y) (ClnY/FnY). They are site-specifically incorporated into the fluorescent flavoprotein iLov[8] (Lov2 domain of *Arabidopsis thaliana* phototropin 2, optimized for fluorescence properties). Critical to the success of the design is the significantly lower pK_a of these genetically encoded FnY and ClnY (from 5.6 to 8.3, Figure 1c) comparing to that of tyrosine (10.2). As a result, these genetically coded UAAs can be selectively deprotonated without deprotonating other tyrosine residues at physiologically relevant pH (4.5−8). We further demonstrate that in anionic state, the phenolate groups of UAAs can donate an electron hundreds of times faster to the photoexcited flavin (FMN*) than the charge neutral UAA or tyrosine, resulting in large fluorescence enhancement (FE) when UAAs are selectively deprotonated or oxidized. In comparison to previously reported FP sensors,[1,5] our sensors exhibit much

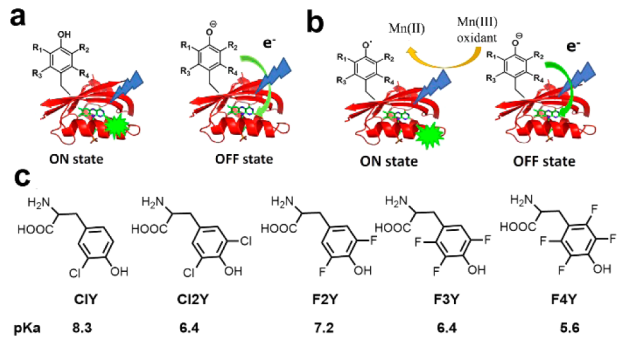

Figure 1. Schematic design of the iLovU PET sensors. (a) The charge-neutral FnY/ClnY are not efficient PET donors, and iLovU protein is in fluorescence ON state. Deprotonation renders the FnY/ClnY UAAs much better PET donors and quench the flavin fluorescence. (b) Oxidation of the FnY/ClnY UAAs blocks the PET quenching pathway and results in iLov fluorescence enhancement. (c) Structure and pK_a of UAAs.

Received: May 26, 2014
Published: September 8, 2014

   dx.doi.org/10.1021/ja505219r | *J. Am. Chem. Soc.* 2014, 136, 13094−13097

larger FE, and more diverse pK_a values matching for the pH of various organelles. Such iLovU PET sensors are also well-suited for investigating the geomicrobiological process of Mn(II) oxidation.[9−11]

The challenge of designing protein PET sensors lies in the site-specific introduction of environmentally sensitive PET probes on suitable fluorescent proteins. We chose to genetically incorporate UAA tyrosine analogues[12−14] as PET probes[15−17] because it has previously been demonstrated that PET rate between a tyrosinate anion and luminophore is hundreds times faster than that of a charge-neutral tyrosine.[16,17] This result can be attributed in part to the fact that while one-electron oxidation of the tyrosine anion is relatively easy (ΔE^0 = 0.71 V), one-electron oxidation of the charge-neutral tyrosine is much more difficult (ΔE^0 = 1.4 V)[17] since the $TyrOH^{\bullet+}$ cation radical (pK_a = −2) is highly unstable.[17] Therefore, efficient ET involving tyrosine residues often requires the coupling of the proton and electron, through proton-coupled electron transfer (PCET). Because a large ΔE^0 difference (0.7 V) exists between the $TyrOH/TyrO^{\bullet+}$ and $TyrO^-/TyrO^{\bullet}$ redox couples, it should be possible to design a fluorophore-spacer-receptor system where ET between the $TyrO^-$ donor and the fluorophore acceptor occurs much faster than fluorescence emission. Protonation or oxidation of $TyrO^-$ results in significant decrease in PET rate, turning on fluorescence. Through this approach, sensors for charged analytes, electro-static field in neurons, and tyrosine post-translational modifications (PTM) may also be designed (Figure S2).[18−20]

To accomplish these goals, we need to choose a fluorescent protein (FP) fluorophore whose excited state is a good electron acceptor for the ClnY/FnY donor. It was shown previously that a tyrosine residue located 4.5 Å away from the flavin in the Fre protein efficiently quenches fluorescence through PET.[15] However, no tyrosine or tryptophan side chain is situated within 7 Å distance to the flavin cofactor in iLov.[8] We therefore chose to install ClnY/FnY on iLov to construct protein PET sensors.

While we and others have previously demonstrated the efficient genetic incorporation of F2Y (pK_a = 7.2) and F3Y (pK_a = 6.4),[21] UAAs which have lower and higher pK_a are needed for PET sensor and enzyme design. To genetically encode ClY, Cl2Y (which are commercially available), and F4Y in *Escherichia coli*, a mutant *Methanococcus jannaschii* tyrosyl amber suppressor tRNA ($MjtRNA^{Tyr}_{CUA}$)/tyrosyl-tRNA synthetase (MjTyrRS) pair was evolved in response to the TAG codon. One MjTyrRS clone emerged for each UAA after three rounds of positive selections and two rounds of negative selections (Table S1) and was named ClYRS, Cl2YRS, and F4YRS, respectively. To unravel the structural basis for the selective recognition of Cl2Y by Cl2YRS, we solved the crystal structures of Cl2YRS, in the presence of Cl2Y (Figure S3).

To determine whether ClYRS, Cl2YRS, and F4YRS can facilitate the incorporation of each UAA into proteins with high efficiency and fidelity, ClYRS, Cl2YRS, and F4YRS were cloned into the pEVOL plasmid[22] for enhanced expression of proteins. An amber stop codon was substituted in the place corresponding to residue Ile486 in the fluorescent protein iLov. Analysis of the purified iLov-486-ClY, iLov-486-Cl2Y, and iLov-486-F4Y by SDS-PAGE showed that full-length iLov proteins were expressed only in the presence of ClY, Cl2Y, or F4Y (Figures S4−5), indicating that ClYRS, Cl2YRS, and F4YRS were specifically active for ClY, Cl2Y, or F4Y, respectively, but inactive for any natural amino acids. ESI-MS analysis of the iLov-486-ClY, iLov-486-Cl2Y, and iLov-486-F4Y mutants gave observed average mass of 13915, 13947, and 13952 Da, respectively, in agreement with the calculated masses (Figure S6).

The UV−vis spectra of both iLov and iLov-486-Cl2Y (hereafter named iLovU2) are characteristic of that of the flavoproteins (Figure S8).[8,23] As pH decreases from 9.0 to 5.0, the iLov and iLovU2 UV−vis spectra have essentially no change in the visible region. While iLov fluorescence (λ_{ex} = 450 nm; λ_{em} = 495 nm) remains unchanged from pH 9.0 to 5.0, iLovU2 fluorescence increases more than 20-fold (Figures S11−13).

Because pH sensors can only be used to accurately measure pH values close to their pK_a, we then designed FP variants with pK_a values matching closely to the pH of different organelles. The apparent pK_a values of the iLovU fluorescence are acutely dependent on specific UAA substitutions at the 486th position and can range from 5.3 to 9.2 (Figure S11). In general, lower pK_a of the UAA in the 486th position corresponds to lower pK_a of the iLovU mutant fluorescence.

We then tested whether iLovU fluorescence can be modulated by mutations around UAA486. Indeed, introduction of the Arg388 mutation (Figure S10) results in a decrease of the pK_a from 6.3 to 5.9, and the Arg388/Arg393 mutation further decreases the pK_a to 5.7, consistent with previous reports that electric field can significantly influence pK_a of nearby tyrosine residues.[18]

If there is photo-induced ET from Cl2Y to flavin in iLovU2, then the Cl2Y radical should be detected. We detected the Cl2Y radical using a tyrosyl radical trapping method (Figure S15).[24] We then investigated the redox property of iLovU2. We added K_2IrCl_6,[25] an one-electron oxidant (E^0 = 0.892 V vs NHE), to iLovU2 and iLov and recorded EPR spectra. As Figure S16 shows, addition of K_2IrCl_6 results in a signal at $g \sim 2$ in iLovU2, but not in iLov. Moreover, addition of K_2IrCl_6 results in a new peak around 400 nm in the UV−vis spectra in iLovU2, but not in iLov (Figure S17). These results indicate that K_2IrCl_6 can selectively oxidize Cl2Y in iLovU2, but not the natural amino acids. Indeed the oxidative peak potential of Cl2Y is 0.83 V vs NHE at pH 7 (Figure S14), significantly less than that of tyrosine.[26] The ability to introduce a radical site-specifically in proteins with such great ease should be useful for probing ET mechanism and dynamic conformation changes in proteins.[15,27]

To resolve the pH and distance dependence of PET between Cl2Y and flavin, the fluorescence lifetime was measured. The fluorescence decay of iLovU2 at pH 5 and 9 fit well to a single-exponential decay. The fluorescence lifetime of iLovU2 mutants, but not iLov, decreased significantly when pH increased from 5 to 9 (Figure 2 and Table S4), which allowed the calculation of k_{ET}.[23] Remarkably, pH increase from 5 to 9 caused a substantial reduction of iLovU2 fluorescence lifetime from 5.0 to 0.2 ns, and the latter corresponds to an ET rate of 4.8×10^9 s^{-1}. We also measured PET rate from Tyr486 to flavin in the iLov-486Tyr mutant and found that the ET rate is more than 100 times slower, at 3.5×10^7 s^{-1}. The ET rates of iLov-393Cl2Y, iLov-391Cl2Y, and iLov-488Cl2Y were slower than iLov-486Cl2Y at 3.8×10^8, 1.1×10^8, and 0.58×10^8 s^{-1}, respectively. Importantly, PET between Cl2Y and flavin can compete with fluorescence when they are separated by relatively long distance (9.6 Å in the case of iLov-488Cl2Y, Figure S7). By contrast, efficient PET between Tyr and flavin requires very short distance (<4.5 Å), and its utility as molecular ruler is limited.[15] The genetically encoded superior PET quenchers are sensitive to subtle distance changes in the angstrom scale and are complementary to the widely adopted FRET technique,[1−4] for the studies on protein conformation dynamics through single-molecule ET.[15]

dx.doi.org/10.1021/ja505219r | J. Am. Chem. Soc. 2014, 136, 13094−13097

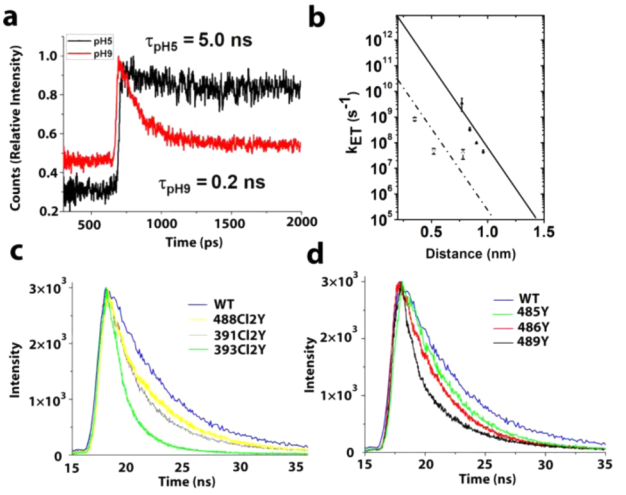

Figure 2. iLov mutant fluorescence: dependence on pH and fluorphore−quencher distance. (a) Fluorescence decay curves of 5 μM iLovU2 in pH 5 or pH 9 buffer, recorded on a streak camera setup, using λ_{ex} = 450 nm and λ_{em} = 500 nm. (b) Plot of k_{ET} vs distance: iLov (open squares); iLovU2 (filled squares). Lines are the best linear fits with a distance-decay constant (β) of 1.4 Å^{-1}. Fluorescence decay curves of 5 μM iLov mutants bearing a Cl2Y mutation (c) or tyrosine mutation (d), carried out on a time correlated single photon counting spectrofluorometer using λ_{ex} = 450 nm and λ_{em} = 500 nm.

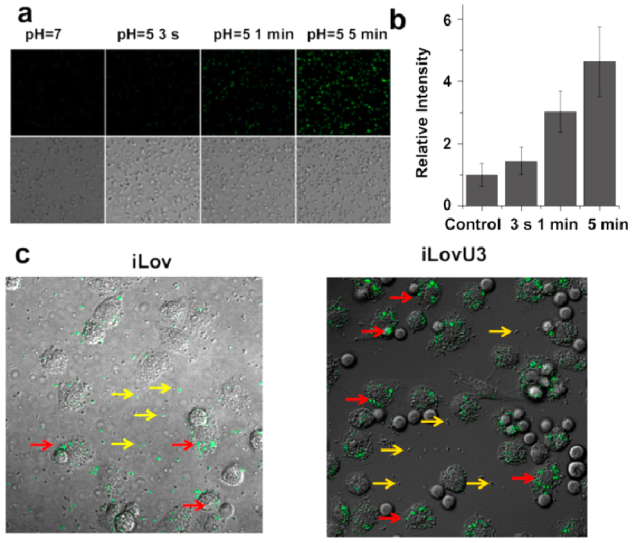

Figure 3. Visualization of pH changes in *E. coli* cells expressing iLovU3. (a) BL21(DE3) *E. coli* cells expressing iLovU3 were visualized by a fluorescence confocal microscope in the fluorescein isothiocyanate (FITC) channel (top) and DIC channel (bottom) at pH 7 and 5. (b) Normalized fluorescence intensity of BL21(DE3) *E. coli* cells expressing iLovU3 were measured by fluorescence plate reader (λ_{ex} = 450 nm; λ_{em} = 495 nm), after incubation in buffers with different pH for indicative times. (c) Visualizing of the *E. coli* phagocytosis. BL21(DE3) *E. coli* cells expressing iLov (left) or iLovU3 (right) were incubated with macrophage cells and then visualized by a fluorescence confocal microscope in the FITC channel. Red arrowheads indicate fluorescent *E. coli* cells after they are phagocytosed by macrophage cells. Yellow arrowheads indicate *E. coli* cells which are not phagocytosed by macrophage cells.

Bacteria rely on elaborate acid resistance system (AR) to survive acidic environment.[28,29] To prevent and treat enteropathogenic bacterial infection, it is important to develop acid turn-on fluorescent sensors to understand bacterial acid resistance mechanism. We tested if the iLov-486Cl2Y388R mutant (pK_a = 5.9, termed iLovU3) could be used for pH sensing *in vivo*. BL21(DE3) *E. coli* cells overexpressing iLovU3 were imaged using a confocal fluorescence microscope at pH 7 and 5. As Figure 3a shows, the cells showed little fluorescence at pH 7. Only 3 s after the pH in the media was dropped to 5 by HCl addition, cellular fluorescence started to increase, reaching maximum in 5 min. These results indicates that in the absence AR systems, *E. coli* cytoplasmic pH decreases rapidly even in mildly acidic conditions. The acid turn-on iLovU sensors may facilitate the discovery of new genes responsible for AR and screening for inhibitors of AR pathways.

We then tested iLovU3's ability to visualize bacteria phagocytosis in macrophage.[28,29] As Figure 3c shows, *E. coli* cells expressing iLov are fluorescent both before and after phagocytosis inside macrophage. By contrast, *E. coli* cells expressing iLovU3 are fluorescent only when they are phagocytosed, but not when they are still moving freely in the medium. Since cytoplasmic acidification is implied as a major killing mechanism of macrophage, our new method may provide the essential tool to identify the key factors required for bacterial engulfment and phagosome maturation.

In addition to imaging pH changes and bacteria phagocytosis, we explored versatility of iLovU as redox sensors. Lignin is the second most abundant biopolymer on Earth, encompassing around 30% of all biomass.[11] However, it is among the most difficult polymers to degrade due to its highly recalcitrant nature. To fully exploit the potentials of biomass as an energy source, we need to design efficient catalysts which can degrade lignin under ambient conditions and convert it into fuels or commodity chemicals. While manganese peroxidase from white rod fungus[11,30] (MnP) is known to oxidized Mn(II) to Mn(III), which then degrades lignin efficiently, the mechanism of biological Mn(II) oxidation remains poorly understood, due to the lack of selective, genetically encoded fluorescent probes for Mn(III). As Figure 4 shows, addition of 10 μM Mn(III) to iLovU2 resulted in more than 8-fold fluorescence enhancement within 1 min, whereas the addition of other transitional metals at 1 mM concentration resulted in no fluorescence intensity change. A linear relationship between fluorescence enhancement and Mn(III) concentration was observed (Figure 4c), and 50 nM Mn(III) can be reliably detected. These results indicate that Mn(III) can selectively oxidize Cl2Y into Cl2Y radical, therefore blocking the PET quenching pathway provided by the Cl2Y anion (Figure 1b). Since MnP is difficult to express in *E. coli*, we have previously engineered a Mn(II) binding site into cytochrome *c* peroxidase (CcP)[30] and show that the resulting mutant (MnCcP) can be expressed in high yield and exhibit manganese peroxidase activity (Figure 4a). As Figure 4b shows, iLovU2 can also detect MnCcP activity, with a 1.8-fold fluorescence enhancement. To the best of our knowledge, this is the first report on a turn-on fluorescence probe for Mn(III). While the Mn(II) oxidation activity of MnCcP is relatively weak, the Mn(III) turn-on iLovU2 sensor should be greatly useful for designing high-throughput screening assays to obtain highly active MnCcP mutants which can be recombinant expressed in high yield.

It was found very recently that Mn(III) is a major component of the sediment redox system.[9] A spectrophotometric protocol was used for the determination of soluble Mn(III). However, Mn(II) and Mn(III) gave rise to the same peak, so toxic cadmium metal ion was needed, and a lengthy procedure was required. By

dx.doi.org/10.1021/ja505219r | *J. Am. Chem. Soc.* 2014, 136, 13094−13097

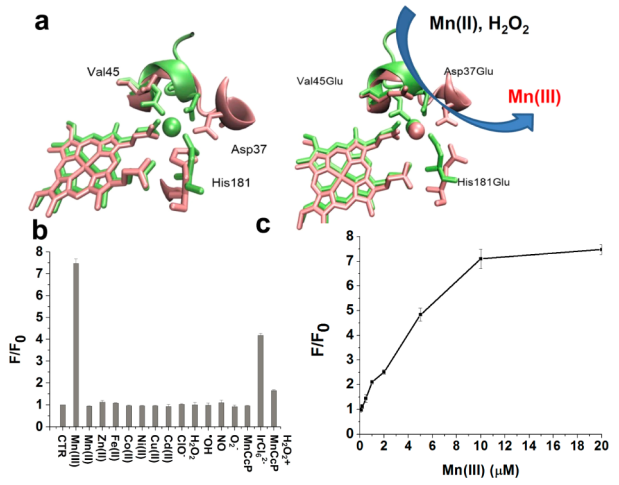

Figure 4. Fluorescence response of iLovU2 to Mn(III). (a) Left: structural overlay of MnP (green, pdb code: 1MNP) and CcP(pink, pdb code: 1CYP); right: structural overlay of MnP (green, pdb code: 1MNP) and MnCcP(pink, pdb code: 2IA8). (b) Fluorescence intensity of iLovU2 (5 μM) was recorded on a Thermo Varioskan Flash fluorescent plate reader, in the presence or absence of 2 mM transition-metal ions or oxidants (10 μM in the case of Mn(III), 100 μM in the case of $IrCl_6^{2-}$, ClO^- and $HO^\bullet$), by exciting the sample at 450 nm and recording the emission at 495 nm. $HO^\bullet$ was generated by reaction of Fe(II) with H_2O_2. Fluorescent intensity in the absence of transition-metal ions was normalized to 1. The oxidation of Mn(II) by MnCcP was also monitored by iLovU2. (c) Fluorescence intensity of iLovU2 (5 μM) in the presence of various concentrations of Mn(III).

contrast, our method allows for the selective detection of Mn(III) within 1 min, without using toxic metal ions or having interference from other metal ions. Our method is potentially useful for the rapid determination of soluble Mn(III) in diverse environmental niches.[10]

In summary, we have developed a novel class of genetically coded PET sensors through the genetic incorporation of UAA Tyr analogs as superior PET quenchers. Our work establishes a platform for many more protein PET sensors which can be rapidly optimized through fluorescence-activated cell sorting, facilitates the *de novo* design of metalloenzymes harboring redox active residues,[31,32] and expands our ability to probe protein conformational dynamics through single-molecule ET.[15]

■ ASSOCIATED CONTENT

Supporting Information

Experiment details, crystal structure of iLovU2 at different pH, UV−vis and fluorescence spectra, CV, EPR spectra. This material is available free of charge via the Internet at http://pubs.acs.org.

■ AUTHOR INFORMATION

Corresponding Author

jwang@ibp.ac.cn

Author Contributions

‖These authors contributed equally.

Notes

The authors declare no competing financial interest.

■ ACKNOWLEDGMENTS

We gratefully acknowledge the Major State Basic Research Program of China (2010CB912301, 2011CBA00800), National Science Foundation of China (91313301, 21325211), CAS grant (KJZD-EW-L01) to J.Y.W.

■ REFERENCES

(1) Newman, R. H.; Fosbrink, M. D.; Zhang, J. *Chem. Rev.* **2011**, *111*, 3614.
(2) Chudakov, D. M.; Matz, M. V.; Lukyanov, S.; Lukyanov, K. A. *Physiol. Rev.* **2010**, *90*, 1103.
(3) Frommer, W. B.; Davidson, M. W.; Campbell, R. E. *Chem. Soc. Rev.* **2009**, *38*, 2833.
(4) Lam, A. J.; St-Pierre, F.; Gong, Y.; Marshall, J. D.; Cranfill, P. J.; Baird, M. A.; McKeown, M. R.; Wiedenmann, J.; Davidson, M. W.; Schnitzer, M. J.; Tsien, R. Y.; Lin, M. Z. *Nat. Methods* **2012**, *9*, 1005.
(5) Miesenbock, G.; De Angelis, D. A.; Rothman, J. E. *Nature* **1998**, *394*, 192.
(6) de Silva, A. P.; Moody, T. S.; Wright, G. D. *Analyst* **2009**, *134*, 2385.
(7) Que, E. L.; Domaille, D. W.; Chang, C. J. *Chem. Rev.* **2008**, *108*, 1517.
(8) Chapman, S.; Faulkner, C.; Kaiserli, E.; Garcia-Mata, C.; Savenkov, E. I.; Roberts, A. G.; Oparka, K. J.; Christie, J. M. *Proc. Natl. Acad. Sci. U. S. A.* **2008**, *105*, 20038.
(9) Madison, A. S.; Tebo, B. M.; Mucci, A.; Sundby, B.; Luther, G. W., III *Science* **2013**, *341*, 875.
(10) Tebo, B. M.; Johnson, H. A.; McCarthy, J. K.; Templeton, A. S. *Trends Microbiol.* **2005**, *13*, 421.
(11) Harms, H.; Schlosser, D.; Wick, L. Y. *Nat. Rev. Microbiol.* **2011**, *9*, 177.
(12) Chin, J. W. *Science* **2012**, *336*, 428.
(13) Liu, C. C.; Schultz, P. G. *Annu. Rev. Biochem.* **2010**, *79*, 413.
(14) Wang, L.; Xie, J.; Schultz, P. G. *Annu. Rev. Biophys. Biomol. Struct.* **2006**, *35*, 225.
(15) Yang, H.; Luo, G. B.; Karnchanaphanurach, P.; Louie, T. M.; Rech, I.; Cova, S.; Xun, L. Y.; Xie, X. S. *Science* **2003**, *302*, 262.
(16) Sjodin, M.; Styring, S.; Akermark, B.; Sun, L. C.; Hammarstrom, L. *J. Am. Chem. Soc.* **2000**, *122*, 3932.
(17) Warren, J. J.; Winkler, J. R.; Gray, H. B. *FEBS Lett.* **2012**, *586*, 596.
(18) Fafarman, A. T.; Sigala, P. A.; Schwans, J. P.; Fenn, T. D.; Herschlag, D.; Boxer, S. G. *Proc. Natl. Acad. Sci. U. S. A.* **2012**, *109*, E299.
(19) Miller, E. W.; Lin, J. Y.; Frady, E. P.; Steinbach, P. A.; Kristan, W. B., Jr.; Tsien, R. Y. *Proc. Natl. Acad. Sci. U. S. A.* **2012**, *109*, 2114.
(20) Lacey, V. K.; Parrish, A. R.; Han, S.; Shen, Z.; Briggs, S. P.; Ma, Y.; Wang, L. *Angew. Chem., Int. Ed.* **2011**, *50*, 8692.
(21) Minnihan, E. C.; Young, D. D.; Schultz, P. G.; Stubbe, J. *J. Am. Chem. Soc.* **2011**, *133*, 15942.
(22) Young, T. S.; Ahmad, I.; Yin, J. A.; Schultz, P. G. *J. Mol. Biol.* **2010**, *395*, 361.
(23) Liu, Z.; Tan, C.; Guo, X.; Li, J.; Wang, L.; Sancar, A.; Zhong, D. *Proc. Natl. Acad. Sci. U. S. A.* **2013**, *110*, 12966.
(24) Bhattacharjee, S.; Deterding, L. J.; Jiang, J.; Bonini, M. G.; Tomer, K. B.; Ramirez, D. C.; Mason, R. P. *J. Am. Chem. Soc.* **2007**, *129*, 13493.
(25) Whittaker, M. M.; Kersten, P. J.; Nakamura, N.; Sanders-Loehr, J.; Schweizer, E. S.; Whittaker, J. W. *J. Bio. Chem.* **1996**, *217*, 681.
(26) Harriman, A. *J. Phys. Chem.* **1987**, *91*, 6102.
(27) Fleissner, M. R.; Brustad, E. M.; Kalai, T.; Altenbach, C.; Cascio, D.; Peters, F. B.; Hideg, K.; Peuker, S.; Schultz, P. G.; Hubbell, W. L. *Proc. Natl. Acad. Sci. U. S. A.* **2010**, *107*, 5693.
(28) Masuda, N.; Church, G. M. *Mol. Microbiol.* **2003**, *48*, 699.
(29) Lu, P.; Ma, D.; Chen, Y.; Guo, Y.; Chen, G.-Q.; Deng, H.; Shi, Y. *Cell Res.* **2013**, *23*, 635.
(30) Pfister, T. D.; Mirarefi, A. Y.; Gengenbach, A. J.; Zhao, X.; Danstrom, C.; Conatser, N.; Gao, Y.-G.; Robinson, H.; Zukoski, C. F.; Wang, A. H. J.; Lu, Y. *J. Biol. Inorg. Chem.* **2007**, *12*, 126.
(31) Winkler, J. R.; Gray, H. B. *Chem. Rev.* **2014**, *114*, 3369.
(32) Hu, C.; Chan, S. I.; Sawyer, E. B.; Yu, Y.; Wang, J. *Chem. Soc. Rev.* **2014**, DOI: 10.1039/C4CS00018H.